African Journal of Advanced Pure and Applied Sciences (AJAPAS)
Online ISSN: 2957-644X
Volume 5, Issue 1, 2026
Page No: 227-234
Website: https://aaasjournals.com/index.php/ajapas/index
ISI 2025: 1.126 SJIFactor 2024: 6.752 معامل التأثير العربي: 1.62

Strength Optimization of Spot Resistance Welded A.H.S.S Dissimilar Thickness by Taguchi Method

Khaled Marwan [1 *], Mohamed Aljadi [2], Maryam Morgham [3] ,
Mohammed Ammar Abuqunaydah [4]
[1,2,3] Libyan Advanced Occupational Center for Welding Technologies, Tripoli, Libya
[4] High vocational Libyan Casting Center, Tripoli, Libya

حسين قوة اللحام النقطي المقاوم للفولاذ المقاوم للصدأ ذي السماكات المختلفة باستخدام طريقة تاجوشي

خالد مروان [1*]، محمد الجدي [2]، مريم مرغم [3] ، محمد عمار محمد أبوقنيدة [4]
[1،2،3] المركز الليبي المتقدم لتقنيات اللحام، طرابلس، ليبيا
[4] المركز العالي الليبي المهني للسباكة، طرابلس، ليبيا

*Corresponding author: khaledgewa@gmail.com

Received: November 17, 2025	Accepted: January 28, 2026	Published: February 09, 2026

Abstract
This study investigates the spot resistance spot welding (SRW) of dissimilar thickness TRIP800 and DP600 steels, which belong to the advanced high strength steel (AHSS) group. Various welding parameters were applied to join these steels, and the optimal weldment strength was targeted through a systematic optimization using the Taguchi method. Tensile shear tests were performed to evaluate the weldment's strength and energy absorption under different welding conditions, which were determined based on the Taguchi L9 orthogonal array design. The results of the optimization process were analyzed using the "the better is the best" approach, with evaluations based on averaging the experimental data. The analysis revealed that welding time is the most significant parameter influencing both weld strength and energy absorption in the dissimilar thickness steels. The welding parameter set that yielded the highest strength, identified by the Taguchi method, closely matched the actual strength values obtained through experimental tests.

Keywords: TRIP800 steel, Taguchi method, Tensile shear strength, welding current, Welding time, Electrode Force.

الملخص
تتناول هذه الدراسة لحام المقاومة النقطية لصلب TRIP800 و DP600 ذي السماكات المختلفة، واللذين ينتميان إلى مجموعة الفولاذ عالي القوة المتقدم (AHSS) طبقت معايير لحام متنوعة لربط هذين النوعين من الفولاذ، وتم استهداف قوة اللحام المثلى من خلال تحسين منهجي باستخدام طريقة تاجوشي. أجريت اختبارات القص الشدي لتقييم قوة اللحام وامتصاص الطاقة في ظل ظروف لحام مختلفة، وفقا لتصميم مصفوفة تاجوشي المتعامدة (L9). حللت نتائج عملية التحسين باستخدام منهجية (الأفضل هو الأنسب)، مع تقييمات مبنية على متوسط البيانات التجريبية. كشف التحليل أن زمن اللحام هو العامل الأكثر أهمية الذي يؤثر على كل من قوة اللحام وامتصاص الطاقة في الفولاذ ذي السماكات المختلفة. تطابقت مجموعة معايير اللحام التي حددتها طريقة تاجوشي باعتبارها تُحقق أعلى قوة بشكل كبير مع قيم القوة الفعلية التي تم الحصول عليها من خلال الاختبارات التجريبية.

الكلمات المفتاحية :فولاذ TRIP800، طريقة تاجوشي، قوة القص الشد، تيار اللحام، زمن اللحام، قوة القطب الكهربائي.

1.Introduction

New generation steels used in the automotive industry to improve fuel economy are known as advanced high strength steels (AHSS) [1–3]. By utilizing these steels, vehicle weight can be reduced through the thinning of cross-sections without compromising strength [4]. A significant portion of the high-strength steel groups employed in automotive applications comprises dual phase (DP) and TRIP steels. These steels are highly effective in absorbing damage caused by accidents, thereby enhancing vehicle safety [5–10]. fuel efficiency and reduce CO2 emissions [2].

Dual phase steels are low carbon steels consisting of a mixture of soft ferrite and hard martensite phases. The unique microstructure provides an excellent combination of strength and ductility. During deformation, ferrite acts as a ductile matrix, while martensite, being a hard phase, impedes dislocation motion. Interestingly, some ferrite can transform into martensite under strain, contributing to strain hardening and enhancing overall hardness [11-16].

Spot resistance welding (SRW) is one of the most widely used welding techniques in the automotive industry due to its speed and adaptability to automation. Several studies in the literature have examined the influence of varying welding parameters—including current intensity, welding time, electrode pressure, holding time, and electrode geometry—on the weld quality and mechanical performance of DP (Dual Phase) and TRIP (Transformation Induced Plasticity) steels. These studies help optimize welding conditions to ensure strong, defect-free joints, especially when working with advanced high-strength steels of differing compositions and properties [17-20].

Improved investigation of the optimization of the spot welding process by examining key parameters, including welding current, welding time, and electrode force, for low-carbon steel. The experiments were conducted using the Taguchi L9 orthogonal array. Their results indicated that the optimal parameters were a welding current of 8 kA, a welding time of 10 cycles, and an electrode force of 2.3 kN. Among these parameters, electrode force was found to have the most significant effect on the welding performance [15].

Recently, it has been observed that research based on the optimization of the mechanical properties of spot resistance welded joints has increased [21-26].

In this study, Taguchi analysis was applied at different welding parameters (welding electrode force, welding time and welding current intensity) to optimize the tensile shear strength and energy absorption of spot resistance welded joints of TRIP800-DP600 steel pairs of different thicknesses. The quality characteristics were analyzed using signal-to-noise (S/N) ratios, and analysis of variance (ANOVA) was conducted to determine the statistical significance and contribution of each welding parameter.

2.Material and methods

The TRIP800-DP600 samples, intended to be joined by spot resistance welding, were prepared by cutting the steel sheets into dimensions of 100 × 30 × 1.5 mm and 100 × 30 × 1.0 mm. The steel strips were joined using a holder mold, overlapping a 30 × 30 mm section. The chemical composition of the steels used is provided in Table 1.

Table1. Chemical composition of the steels used in the experimental study (%weight).

	C	Si	Mn	Cr	Mo	Al	Fe
DP600	0,13	0,35	1,426	0,637	0,013	0,053	Rest
TRIP800	0,2	1,66	1,69	0,006	0,011	0,43	Rest

2.2 Resistance Spot Welding:

The joining process was carried out using a 60 kVA BAYKAL SP60 brand electronic current and time-controlled AC spot resistance welding machine, equipped with pneumatic pressure. The SRW setup is illustrated in Figure 1. The welding current intensity, welding time, and electrode force parameters, which were used for Taguchi analysis, were determined by selecting the optimal values from the results of preliminary experimental studies. These welding parameters are provided in Table 2. Holding time and electrode pressure force were set to 15 cycles (1 cycle = 0.02 sec) and 6 kN for all joints. A spherical-head F16 type electrode (Cu-Cr-Zr) was employed in the experiments with a 5.5 mm diameter were utilized. The spherical end of the Cu–Cr–Zr spot resistance welding (SRW) electrode was water cooled. The electrode dimensions and corresponding macrograph are presented in Figure 2**.**

Figure 1. The spot welding machine used in this study.

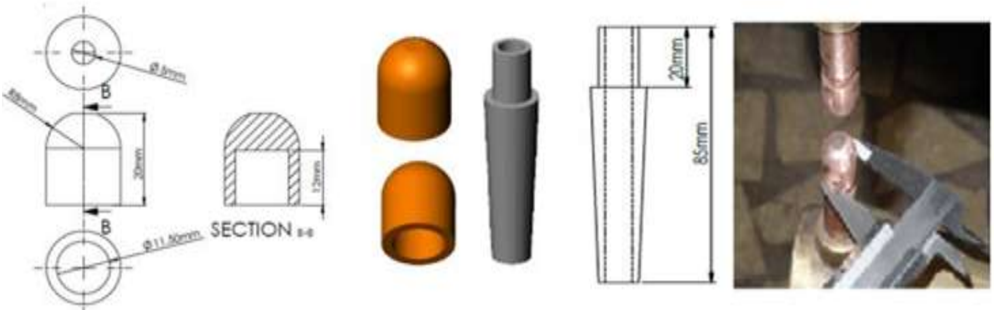

Figure 2. The dimensions and macrograph of spherical tip Cu-Cr-Zr electrodes.

2.3 Tensile Shear Test:
To experimentally evaluate the effects of welding parameters on the strength and energy absorption of the joints, an additional 3 pairs of tensile shear test samples were included alongside the 5 samples from previous studies. This was done to enhance the reliability of the results. The dimensions of the tensile shear test specimens are shown in Figure 3 (a) and (b), respectively. In total, 8 tensile shear tests were conducted for each test parameter were prepared according to DIN EN ISO 14272 standards., and the average tensile shear strengths and energy absorptions were calculated using the device's current program. The welded material pairs were subjected to tensile shear testing until failure in a SHIMADZU brand tensile testing machine, having about 50 KN capacity as shown in the figure 4, with a tensile speed set to 5 mm/min.

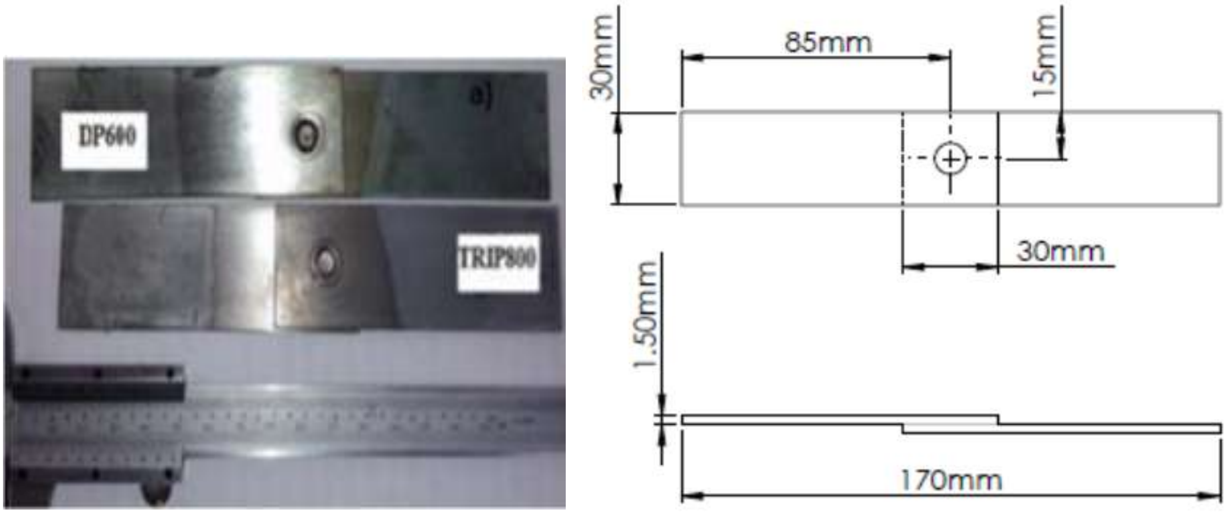

a

b

Figure 3. a. The joined tensile shear. b. The dimension of the tensile shear test sample.

Figure 4. The tensile test machine used for testing processes.

2.4. Experimental Design:
This study aimed to determine the optimal tensile shear strength and energy absorption by selecting the most suitable welding parameters using the Taguchi method. The selected welding parameters (factors) and their levels are presented in Table 2.

Table 2. Test parameters for the steel pair of different thicknesses and their values at each level.

Sheet thicknesses	Symbol	RSW parameters	Unit	Level 1	Level 2	Leve.3
1 mm-1.5 mm	A	Electrode Force	KN	4	5	6
	B	Welding Current	KA	5	7	9
	C	Welding time	cycle	15	20	25
1 cycle =0.02 s						

Considering the welding parameters listed in Table 2, the Taguchi L9 orthogonal array, comprising nine experiments, was selected as the most suitable design for this study. Optimization using the Taguchi method was carried out with the aid of Minitab 21 software.

2.5. Analysis with Taguchi Method:
This study aims to achieve the highest possible tensile shear strength and energy absorption in spot resistance welded joints. Accordingly, the 'larger-is-better' criterion was adopted, and Equation (1) was used to calculate the signal-to-noise (S/N) ratios [23-26]. In this equation, y_i represents the observed data from each experiment, and n denotes the number of experiments. The measured values of tensile shear strength (kN) and energy absorption (J), obtained according to the L9 orthogonal array, were converted into S/N ratios and expressed in decibels (dB), as presented in Table 3.

$$S/N = -10\log\left(\frac{1}{n}\sum_{i=1}^{n}\frac{1}{y_i^2}\right), \quad i=1,2 \ldots k \tag{1}$$

Table 3. Tensile shear strength, energy absorption, and S/N ratios for Taguchi L9 experiments.

No.	Welding parameters			Tensile shear strength (kN)	S/N Rate (dB)	Energy Absorption (J)	S/N Rate (dB)
	Electrode Force	Welding Current	Welding time				
1	4	5	15	11.50	21.5836	37	31.3640
2	4	7	20	12.26	21.7272	40	32.0412
3	4	9	25	13.25	22.4115	45	33.0643
4	5	5	20	12.47	21.72.72	38	31.5957
5	5	7	25	12.37	21.7981	39	31.8213
6	5	9	15	11.95	21.5836	37	31.3640
7	6	5	25	11.50	21.9382	41	32.2557
8	6	7	15	11.92	21.5109	33	30.3703
9	6	9	20	12.41	21.8684	39	31.8213

3. Experimental Result

3.1. Analysis of Experimental Results:

The average signal-to-noise (S/N) ratio graphs for tensile shear strength and energy absorption corresponding to each welding parameter are presented in Figures 5 a and b, respectively. According to the Taguchi optimization method, the factor level with the highest S/N ratio indicates the optimal condition for the corresponding performance characteristic [23-26]. Table 4 summarizes the average S/N ratios, the overall mean S/N ratio, and the Delta values, which represent the differences between the maximum and minimum S/N ratios for each parameter.

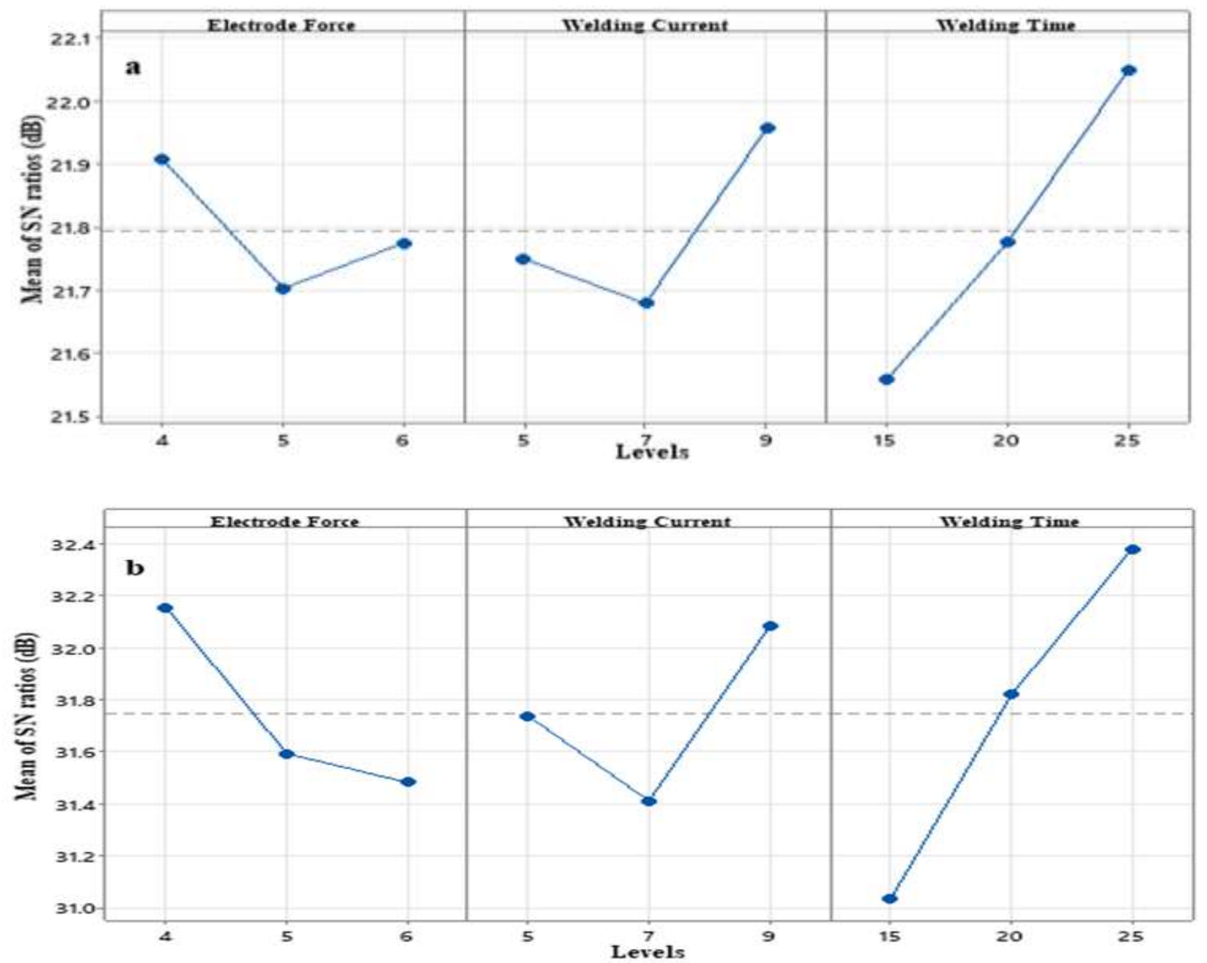

Figure 5. a) Tensile shear strength, b) S/N ratios of welding parameters for energy absorption values.

Table 4. Average S/N ratios

Results	Symbol	RSW parameters	Unit	S/N ratio			Total ratio.S/N (dB)	Delta
				Level 1	Level 2	Level 3		
Tensile shear strength (kN)	A B C	Electrode Force Welding Current Welding time	KN KA cycle	21.91* 21.75 21.56	21.70 21.68 21.77	21.77 21.95* 22.05*	21.79	0.20 0.28 0.49
Energy Absorption (J)	A B C	Electrode Force Welding Current Welding time	KN KA cycle	32.16* 31.74 31.03	31.59 31.41 31.82	31.48 31.82* 32.38*	31.63	0.67 0.67 1.35

Not: * optimum level

An examination of the graphs in Figures 1a and 1b, along with the optimal S/N ratio levels presented in Table 4 for both tensile shear strength and energy absorption, reveals that the highest values are achieved at Level 1 for electrode pressure force, Level 3 for welding current, and Level 3 for welding time. Accordingly, the optimal combination of welding parameters for maximizing tensile shear strength and energy absorption is determined to be A1B3C3.

3.2. Analysis of Variance (ANOVA):

The ANOVA results for tensile shear strength and energy absorption are presented in Tables 5 and 6, respectively. These tables display the sum of squares (SS), mean square values (MS), F-values, and percentage contribution rates (PCR) for each parameter. The degrees of freedom (DF) associated with each variable are also included, indicating the extent of influence each factor has on the results.

Table 5. Analysis of variance for tensile shear strength S/N ratios.

Thickness	Variable	DF	SS	MS	F-value	PCR
(1.5mm-1mm)	Electrod Force (KN)	2	0.14000	0.7000	1.75	11.47
	Welding Current (KA)	2	0.26000	0.13000	3.25	21.32
	Welding Time (Cycle)	2	0.74000	0.37000	9.25	60.65
	Error	2	0.08000	0.04000		6.56
	Total	8	1.22000			100

Table 6. Analysis of variance for energy absorption S/N ratios.

Thickness	Variable	DF	SS	MS	F-value	PCR
(1.5mm-1mm)	Electrod Force (KN)	2	16.222	8.1111	10.43	18.96
	Welding Current (KA)	2	13.556	6.7778	8.71	15.84
	Welding Time (Cycle)	2	54.222	27.1111	34.86	63.40
	Error	2	1.556	0.7778		1.80
	Total	8	85.556			100

An examination of the tables reveals that welding time is the most influential parameter on tensile shear strength, with a contribution of 60.65%, followed by welding current at 21.32%. The electrode pressure force was found to have a lesser effect, contributing 11.47% to the tensile shear strength of the joints.
Considering the energy absorption capacities of the test samples, it was determined that the highest effect was on welding time with 63.40%, followed by electrode pressure force with 18.96% and then welding current with 15.84%. Accordingly, while the most effective welding parameters determined for the tensile shear strength and energy absorption values of steel pair spot welding joints of different thicknesses are welding time, the effect rates of other factors have varied. While the second most effective parameter affecting the tensile shear strength is welding time, it is seen that the second most effective parameter for energy absorption values is the electrode pressure force.

3.3. Validation Experiments

According to the Taguchi method, once the optimal parameter levels are estimated, the accuracy of the optimization is typically validated through confirmation (verification) experiments. However, if the estimated optimal levels correspond to one of the experimental trials conducted before optimization, the performance of the optimization can be evaluated without additional confirmation experiments [23-26]. In this study, the estimated optimal levels for both tensile shear strength and energy absorption were included among the original experimental runs.
A comparison of the predicted and experimental results is presented in Table 7. When the S/N ratios and the differences between the predicted values and the verification experiment results for tensile shear strength and energy absorption are examined, the discrepancy is found to be minimal (less than 0.2). This confirms that the Taguchi optimization method is a simple, reliable, and effective approach for determining the performance characteristics of welding outputs.

Table 7. Validation test results.

	Optimum parameters		Differences
	Predicted	Experimental	
Level	A1B3C3	A1B3C3	
Tensile shear strength (kN)	13.0667	13.2	0.1333
S/N Ratio (dB)	22.3226	22.4115	0.0889
Level	A1B3C3	A1B3C3	
Energy Absorption (J)	45.1111	45.0	0.1111
S/N Ratio (dB)	33.1317	33.0643	0.06749

4. Conclusions:

The findings obtained in this analysis study can be summarized as follows:

- The Taguchi L9 orthogonal array design was successfully applied to optimize the spot resistance welding process parameters for joining TRIP800-DP600 steel sheets of different thicknesses. This approach enabled efficient experimentation with a reduced number of trials.
- As a result of Taguchi optimization, it was found that the most effective welding parameter in optimizing the tensile shear strength of TRIP800-DP600 different types of steel joints with different thicknesses was welding time with 60.65%, and the next effective parameter was welding current with 21.32%. Among the welding parameters, the effect of electrode pressure force was found to be less effective than the other two, at 11.47%.
- For optimizing energy absorption capacity, welding time again showed the highest influence with 63.40%, followed by electrode pressure force at 18.96%, and welding current at 15.84%.
- An examination of the average S/N ratio graphs for both tensile shear strength and energy absorption indicates that the optimal parameter levels are identical for both characteristics, identified as A1B3C3.
- The optimization results show strong agreement with the experimental data.

Compliance with ethical standards

Disclosure of conflict of interest

The authors declare that they have no conflict of interest.

References

[1] F. Öztürk, S. Toros, E. Esener, E. Uysal: Otomotiv Endüstrisinde Yüksek Mukavemetli Çeliklerin Kullanımının İncelenmesi, Mühendis ve Makina, 50 (586) (2009) pp. 44-45.

[2] Hayder H. Khaleel, Ibtihal A. Mahmood, and Fuad Khoshnaw. Optimization process of resistance spot welding for high-strength low-alloy steel using Taguchi method, Open Engineering 2022; 12: 680–690.

[3] S. Brawser, L.A. Pepke, G. Weber, M. Rethmeier: Deformation Behavior Of Spot Welded High Strength Steels for Automotive Applications, Mater Sci Eng. A, 527 (2010) pp.7099-7108.

[4] D.W. Zhao, Y.X. Wang, S. Shang, Z. Lin: Multi-Objective Optimal Design of Small Scale Resistance Spot Welding Process with Principal Component Analysis And Response Surface Methodology, J. Intell Manuf. 26 (2013) pp.1-14.

[5] G. Song, T. Vystavel, N. Vander Pers, J.T.M. de Hassan, W. Sloof: Relation Between Microstructure and Adhesion of Hot Dip Galvanized Zinc Coatings on Dual-Phase Steel, Acta Mater, 60 (2012) pp. 2973-2981.

[6] R. Lagneborg: New Steels and Steel Applications for Vehicles, Materials and Design, 12 (1991) pp. 3-14.

[7] H. Hayashi, T. Nokagawa: Recent Trends in Sheet Metals and Their Formability In Manufacturing Automotive Panels, J. Materials Processing Technology, (1994) pp. 455-487.

[8] K. Mari, S. Maki, Y. Tanoka: Warm and Hot Stamping of Ultra High Tensile Strength Steel Sheets Using Resistance Heating CIRP Analyst, Manufacturing Technology, 54 (2005) pp. 209-212.

[9] International Iron and Steel Institute, Project Reports on Ultra Light Steel Auto Body, (2006).

[10] C.W. Zhang, D. Raabge: Interaction Between Recrystallization and Phase Transformation During Intercritical Annealing Cold-Rolled Dual-Phase Steel: A Cellular Automation Model, Acta Mater, 60 (2012) pp. 5504-5517.

[11] Z. Yinghui, M. Yonli, K.Yonglin, Y. Hao: Mechanical Properties And Microstructure of TRIP Steels Produced Using TSCR Process, Journal of University of Science and Technology, Beijing, 13 (5) (2006) pp. 416-421.

[12] D. Wu, L. Zhuang, L. Hui-sheng: Effect of Controlled Cooling After Hot Rolling On Mechanical Properties of Hot Rolled TRIP Steel, Journal of Iron and Steel Research International, 15 (2) (2008) pp.65-70.

[13] S. Koh-Ichi, M. Toshiki, H. Shun-Ichi, M. Yoichi: Formability of Nb Bearing Ultra High Strength TRIP-Aided Sheet Steels, Journal of Materials Processing Technology, 177 (1) (2006) pp.390–395.

[14] L. Skoalova, R. Divišová, D. Jandová: Thermo-Mechanical Processing of Low-Alloy TRIP Steel, Journal of Materials Processing Technology, 175 (1) (2006) pp.387–392.

[15] S. Wen, L. Lin, B.C.D. Cooman, P. Wollants, C. Yang: Thermal Stability of Retained Austenite in TRIP Steel After Different Treatments, Journal of Iron and Steel Research, International, 15 (1) (2008) pp. 61-64.
[16] L. Zhuang, W. Di, H. Rong: Austempering of Hot Rolled Si-Mn TRIP Steels, Journal of Iron and Steel Research International, 13(5) (2006) pp. 41-46.
[17] M.I. Khan, M.L. Kuntz, Y. Zhou: Effects of Weld Microstructure on Static and Impact Performance of Resistance Spot Welded Joints in Advanced High Strength Steels, Sci Technol. Weld Join. 13 (2008) pp. 294-304.
[18] X. Sun, E.V. Stephens, M.A. Khaleel: Effects of Fusion Zone Size and Failure Mode on Peak Load and Energy Absorption of Advanced High Strength Steel Spot Welds Under Lap Shear Loading Conditions, Eng. Fail Anal.15 (2008) pp. 356–67.
[19] J.D. Radakovic, M.D. Tumuluru: Proceeding of the International Sheet Metal Welding Conference XIII, (2008).
[20] O. Kwon, S.C. Baik: Manufacture and application of advanced high strength steel sheets for auto parts manufacture, Pohang: POSCO (2005) pp. 785–90.
[21] M. Pouranvari, S.P.H. Marashi, D.S. Safanama: Failure Mode Transition in AHSS Resistance Spot Welds. Part II: Experimental investigation and model validation, Materials Science and Engineering: A, 528 (29–30) (2011) pp. 8344–8352.
[22] G. Thakur, T.E. Rao, M.S. Mukhedkar, V.M. Nandedkar: Application of Taguchi Method for Resistance Spot Welding of Galvanized Steel, ARPN Journal of Engineering and Applied Sciences 5(1) (2010) pp. 22-26.
[23] M. Günay, E. Yücel, "Application of Taguchi method for determining optimum surface roughness in turning of high-alloy white cast iron", Measurement, 46: 913–919 (2013).
[24] S. Chaudhary, V.K. Sharma, K. Rana: International Journal of Enhanced Research in Science Technology & Engineering, 3(10) (2014) pp.217-221.
[25] N. Muhammad, Y.H. P Manurung, M. Hafidzi, S.K. Abas, Ghalib Tham, E. Haruman: Optimization and Modeling o Spot Welding Parameters with Simultaneous Multiple Response Consideration Using Multi-Objective Taguchi Method and RSM, Journal of Mechanical Science and Technology 26 (8) (2012) pp. 2365-2370.
[26] A.G. Thakur, T.E. Rao, M.S. Mukhedkar, V.M. Nandedkar: Application of Taguchi Method For Resistance Spot Welding Of Galvanized Steel, ARPN Journal of Engineering and Applied Sciences 5(11) (2010) pp. 22-26.
[27] Word Auto steel, Advanced High Strength Steel (AHSS) Application Guide Lines, 4th ed., http://www.wordautosteel.org, (2009).

